

# Analysis of negative magnetoresistance. Statistics of closed paths. I. Theory

G. M. Minkov, A. V. Germanenko,\* V. A. Larionova and S. A. Negashev  
*Institute of Physics and Applied Mathematics, Ural State University  
620083 Ekaterinburg, Russia*

I. V. Gornyi  
*A. F. Ioffe Physical-Technical Institute, 194021 St. Petersburg, Russia  
(September 26, 2018)*

Statistics of closed paths in two-dimensional (2D) systems, which just determines the interference quantum correction to conductivity and anomalous magnetoconductance, has been studied by computer simulation of a particle motion over the plane with randomly distributed scatterers. Both ballistic and diffusion regimes have been considered. The results of simulation have been analyzed in the framework of diffusion approximation. They are used for calculation of the magnetic field dependence of magnetoconductance in the model 2D system. It is shown that the anomalous magnetoconductance can be in principle described by the well known expression, obtained in the diffusion approximation, but with the prefactor less than unity and phase breaking length which differs from true value.

PACS numbers: 73.20.Fz, 72.20.Dp, 72.10.-d

## I. INTRODUCTION

It is well known that the interference of electron waves scattered along closed trajectories in opposite directions produces a quantum correction to the conductivity. An external magnetic field applied perpendicular to the two-dimensional (2D) layer destroys the interference and suppresses the quantum correction. This results in anomalous negative magnetoresistance, which is experimentally observed in many 2D systems. This phenomenon can be described in the framework of quasiclassical approximation which is justified under the condition  $k_F l \gg 1$ , where  $k_F$  is the Fermi wave vector,  $l$  is the mean free path. In this case the conductivity correction is usually expressed through the classical quasiprobability for an electron to return to the area of the order  $\lambda_F l$  ( $\lambda_F = 2\pi/k_F$ ) around the start point<sup>1-4</sup>

$$\delta\sigma = -\sigma_0 \frac{\lambda_F l}{\pi} W, \quad (1)$$

where  $\sigma_0 = e^2 k_F l / (2\pi\hbar)$ , and  $W$  stands for the quasiprobability density of return (*quasi-* means that  $W$  includes not only the classical probability density, but the effects of interference destruction due to an external magnetic field and inelastic scattering processes). In order to calculate a magnetic field dependence of negative magnetoresistance the quasiprobability  $W$  is represented as a sum of contributions of closed paths with  $N$  collisions,  $W_N$ . Then, Eq. (1) can be rewritten as

$$\delta\sigma = -2\pi l^2 G_0 \sum_{N=3}^{\infty} W_N, \quad (2)$$

where  $G_0 = e^2 / (2\pi^2\hbar)$ . Here, only paths with  $N \geq 3$  are taken into account, because the paths with  $N = 1, 2$

have zero areas and their contributions are not influenced by the magnetic field.

The expression (2) for backscattering quantum correction is true for an arbitrary magnetic field, any anisotropy of scattering and distribution of scatterers, and various relationship between phase and momentum relaxation times,  $\tau_\varphi$  and  $\tau$ , respectively. The sum (2) is usually calculated by means of diagrammatic technique.<sup>5,6</sup> Analytical expressions for negative magnetoresistance have been obtained this way for random distribution of scatterer in the following cases (i) arbitrary scattering anisotropy for low magnetic field  $B < B_{tr}$ ,<sup>7</sup> where  $B_{tr} = \hbar c / (2el^2)$ ; (ii) isotropic scattering for  $B \gg B_{tr}$ .<sup>4</sup> In the diffusion approximation, i. e. when the number of collisions for actual trajectories is much greater than unity, this procedure gives<sup>5</sup>

$$\begin{aligned} \Delta\sigma(b) &= \delta\sigma(b) - \delta\sigma(0) \\ &= aG_0 \left[ \psi\left(\frac{1}{2} + \frac{\gamma}{b}\right) - \psi\left(\frac{1}{2} + \frac{1}{b}\right) - \ln\gamma \right], \quad (3) \end{aligned}$$

where  $\gamma = \tau / \tau_\varphi$ ,  $b = B / ((1 + \gamma)^2 B_{tr})$ ,  $\psi(x)$  is a digamma function, and  $a$  is so called prefactor, which is equal to unity according to the theory. For  $x \gg 1$   $\psi(1/2 + x) \simeq \ln(x)$ , and the expression (3) coincides with that obtained in Ref. 6. The calculations of  $\delta\sigma(b)$  beyond the diffusion limit<sup>3,5</sup> show that  $\delta\sigma(b)$  markedly deviates from this theory if the number of collisions for actual trajectories is not very large. The role of nonbackscattering contribution to magnetoconductance has been studied in Ref. 4. This contribution has been found to cause the reduction of scattering at arbitrary angles and, in contrast to the coherent backscattering, the conductivity increasing. In the diffusion limit the nonbackscattering contribution is

negligible small, but in the case of a strong magnetic field  $B > B_{tr}$  it should be taken into account.

It is usual to analyze experimental data by means of equation (3). If this equation describes the magnetic field dependence of negative magnetoresistance satisfactorily, it is possible to determine  $\tau_\varphi$  and its temperature dependence.

In our two papers presented back-to-back we put forward a new approach to calculation and analysis of negative magnetoresistance. By representing the quasiprobability  $W$  as a sum of contributions from trajectories with given areas we express the negative magnetoresistance in terms of area distribution function of closed paths  $W(S)$  and area dependence of their average lengths  $\bar{L}(S)$ . It is shown that these are precisely the statistic characteristics which can be obtained from the analysis of experimental data (see the following paper). In the present paper the statistics of closed paths is studied theoretically by using computer simulation. This method allows to obtain the statistic characteristics of closed paths beyond the diffusion approximation without any restriction on the scattering anisotropy and impurity distribution when analytical expressions cannot be derived.

This paper is organized as follows. In the next section we give the necessary formulas and definitions. In Section III the details of simulation procedure are presented. The statistics of closed paths obtained from the simulation is given in Section IV. The results are compared with those obtained in the framework of the diffusion theory. In Section V the magnetic field dependence of negative magnetoresistance of the model 2D system are presented and analyzed. Both coherent backscattering and non-backscattering contributions to magnetoconductance are considered.

## II. BASIC EQUATIONS

Let us introduce the value  $w_N(S)$  in such a way that  $w_N(S)dS$  gives the probability density of return after  $N$  collisions following a trajectory, which encloses the area in the range  $(S, S + dS)$ . In this case Eq. (2) for conductivity correction in a magnetic field is written as follows

$$\delta\sigma(b) = -2\pi l^2 G_0 \times \sum_{N=3}^{\infty} \int_{-\infty}^{\infty} dS w_N(S) \cos\left(\frac{(1+\gamma)^2 bS}{l^2}\right). \quad (4)$$

In order to take into account inelastic processes destroying the phase coherence we include the factor  $\exp(-L/l_\varphi)$  in Eq. (4), where  $l_\varphi$  is the phase breaking length connected with  $\tau_\varphi$  through the Fermi velocity,  $l_\varphi = v_F \tau_\varphi$  and replace the summation over  $N$  by integration over the path length  $L$ . Then, Eq. (4) takes the form

$$\delta\sigma(b) = -2\pi l^2 G_0 \int_0^{\infty} \frac{dL}{l} \left\{ \exp\left(-\frac{L}{l_\varphi}\right) \right.$$

$$\left. \int_{-\infty}^{\infty} dS w(S, L) \cos\left(\frac{(1+\gamma)^2 bS}{l^2}\right) \right\}. \quad (5)$$

Here,  $w(S, L)dS$  gives the density probability of return along a trajectory with the length  $L$  and area in the interval  $(S, S + dS)$ . Let us introduce the average length  $\bar{L}$  of closed paths with a given area in such a way:

$$\exp\left(-\frac{\bar{L}(S)}{l_\varphi}\right) = \frac{1}{W(S)} \times \int_0^{\infty} \frac{dL}{l} w(S, L) \exp\left(-\frac{L}{l_\varphi}\right), \quad (6)$$

where

$$W(S) = \int_0^{\infty} \frac{dL}{l} w(S, L). \quad (7)$$

In this case Eq. (5) can be rewritten as follows

$$\delta\sigma(b) = -2\pi l^2 G_0 \int_{-\infty}^{\infty} dS \left\{ W(S) \exp\left(-\frac{\bar{L}(S)}{l_\varphi}\right) \cos\left(\frac{(1+\gamma)^2 bS}{l^2}\right) \right\}. \quad (8)$$

Thus, the area distribution function  $W(S)$  and function  $\bar{L}(S)$  play a decisive part in the magnetic field dependence of  $\delta\sigma$ . It is clearly seen that these functions can be extracted from experimental  $\delta\sigma(b)$  curves by using Fourier transformation. To understand what these statistic characteristics are let us turn now to theoretical study of statistics of closed paths through the computer simulation of a particle motion over 2D plane with randomly distributed scatterers.

## III. SIMULATION DETAILS

The model 2D system is conceived as a plain with randomly distributed scattering centers with a given total cross-section. It is represented as a lattice  $M \times M$ . The scatterers are placed in a part of the lattice sites with the use of a random number generator. We assume that a particle moves with a constant velocity along straight lines which happen to be terminated by collisions with the scatterers.<sup>8</sup> The following algorithm has been realized in computer to obtain the information about the statistics of closed paths:

1. A start point is chosen to coincide with some scatterer near the center of the lattice;
2. We consider a particle suffers the first collision in the start point and begins to move in a random direction (see inset in Fig. 1);
3. If the particle passes in the vicinity of some scatterer at a distance less than  $s/2$ , where  $s$  is the total cross-section of the scatterer, the collision is considered to take place;

4. Then a scattering angle is randomly generated and the particle begins to move in the new direction until the next collision occurs. The distances between two sequential collisions are stored in order to calculate the mean free path;
5. If the trajectory of the particle passes near the start point at the distance less than  $d/2$  (where  $d$  is a prescribed value, which is small enough), it is perceived as being closed. Its length  $L$ , the number of collisions  $N$ , the angle  $\theta$  between the first and the last segments of the trajectory, and the enclosed algebraic area, calculated according to

$$S = \sum_{j=1}^{N-1} \frac{y_{j+1} + y_j}{2} (x_{j+1} - x_j) + \frac{y_N + y_1}{2} (x_N - x_1), \quad (9)$$

where  $x_j, y_j$  stand for coordinates of  $j$ -th collision, are kept in memory. Then, the particle continues moving in the same direction. Notice that multi-returned trajectories are taken into account. Their length and area are calculated beginning with the start point;

6. Steps 3–5 are repeated until the particle goes out of the lattice or a number of collisions exceeds some large prescribed value  $N_m$ ;
7. Then, another particle is launched from the start point in a random direction, and steps 3–6 are repeated;
8. After a thousand of starts, a new start point is chosen, and steps 2–7 are repeated, for tens of times;
9. Then a new ensemble of scatterers is randomly generated and the whole procedure is done over and over again.

The procedure described allows to find the probability,  $\mathcal{T}$ , for the trajectory to pass at a distance less than  $d/2$  near the start point, instead of the probability density of return,  $W$ , which stands in Eq. (1). But it can be shown (see Appendix) that for  $d \ll l$  these values are connected through the simple relationship  $W = (dl)^{-1}\mathcal{T}$ .

All the results presented in the paper have been obtained using the following parameters: the lattice dimension is  $6500 \times 6500$ , the total number of scatterers is about  $8 \times 10^4$ ,  $N_m = 10^3$ ,  $s = 7$ , and  $d = 1$  (hereafter all the lengths and areas are given in units of lattice parameter and lattice parameter squared, respectively). The total number of starts,  $I_s$ , is about  $10^6 - 10^7$ . The mean free path computed for such a system is 77.8. It is close to theoretical estimation of mean free path  $l = (N_s s)^{-1}$ , where  $N_s$  is a density of scatterers. The calculations were carried out also with other parameters  $M$  and  $s$  differed 2–3 times. It has been shown that this leads only to a

change in the value of  $l$ , but does not influence the dependence of magnetoconductance on the reduced magnetic field  $b = B/B_{tr}$ .

In order to illustrate the 2D system which can correspond to our model in reality, let us set the lattice constant equal to 0.5 nm. In this case our model provides an example of 2D system with the concentration of scatterers  $7.5 \times 10^{11} \text{ cm}^{-2}$ , mean free path  $l = 38.9 \text{ nm}$ , and  $B_{tr} \simeq 0.2 \text{ T}$ .

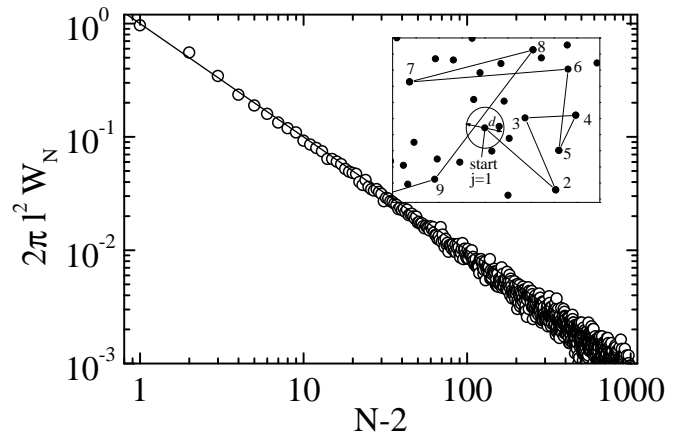


FIG. 1. The quantity  $2\pi l^2 W_N$  as a function of collision number  $N$ . Circles are the result of simulation. The line is theoretical calculation using Eq. (10). The inset shows schematically one of the paths which pass through the start point vicinity after  $N = 8$  collisions.

## IV. STATISTICS OF CLOSED PATHS

### A. Simulation results

It has been shown in Ref. 3 that if we decompose the probability density of return to the origin  $W$  as a sum of contributions of paths with  $N$  collisions,  $W_N$ , for each partial contribution a simple expression is valid:

$$2\pi l^2 W_N = (N - 2)^{-1}, \quad N \geq 3. \quad (10)$$

We emphasize that Ex. (10) is exact. It has been obtained for random distribution of scatterers of zeroth radius. Corresponding simulation results for our model system are presented in Fig. 1. As is clearly seen the power law works well in the whole range of  $N$ . The value of  $W_N$  is really proportional to  $(N - 2)^\alpha$  with  $\alpha = (-1.05 \pm 0.02)$  which is close to the theoretical value  $\alpha = -1$ . The slight difference results from a specific feature of our system. The matter is that the scatterers are placed discretely rather than continuously as in the theoretical approach. They cannot lie closer than one unit cell of the lattice. This leads to the fact that unlike the theory a distance between two sequential collisions in our model is always greater than some critical value of the order of lattice constant. From this point of view, our model system most closely corresponds to real 2D system, where the ionized

impurity distribution is discrete and correlated to some extent due to Coulomb repulsion at growth temperature. It is easy to show in the framework of theoretical approach Ref. 3 that the cutoff of short free paths results in more steep  $W_N(N)$  relationship as compared with Eq. (10).

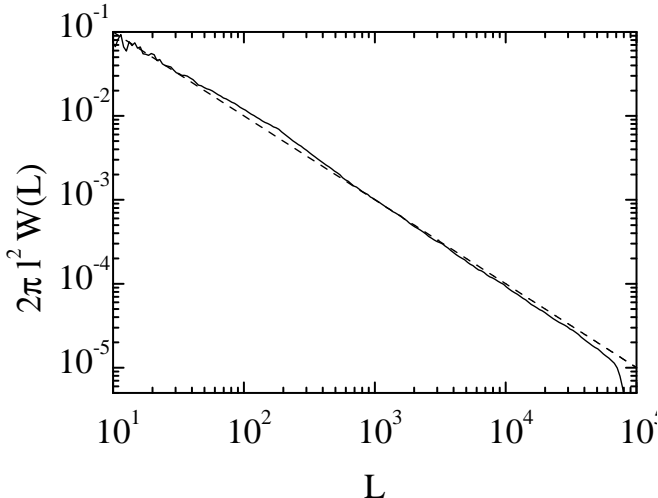


FIG. 2. Length distribution function of closed paths  $W(L)$ . The solid curve is the result of simulation, the dotted curve shows  $L^{-1}$  function.

The length distribution function for closed paths,  $W(L)$ , is presented in Fig. 2. The function  $W(L)$  is defined in such a way that the value  $W(L)dL$  is the probability density of return to the origin following a trajectory with the length belonging to the interval from  $L$  up to  $L+dL$ . As is seen  $W(L)$  is inversely related to trajectory length. A drastic decrease of  $W(L)$  for  $L \gtrsim 7.5 \times 10^4$  results from the restriction on maximal number of collisions per one trajectory in our algorithm. As a consequence of this restriction the probability of a closed path to have the length exceeding the value  $N_m l \simeq 8 \times 10^4$  is negligible small.

Figure 3 shows the area distribution function obtained from our numerical simulation. Since the results of calculations are identical for positive and negative algebraic areas, hereafter we present theoretical curves in the positive area range only. It is reasonable that  $W(S)$  is a diminishing function. As is seen it is difficult to describe  $W(S)$  curve by a power function in the whole range of areas. However, for large  $S$  the power function  $S^{-1}$  is a good asymptotic of  $W(S)$ .

The results of our calculation of  $\bar{L}(S)$  for different values of  $l_\varphi$  are presented in Fig. 4. As is seen the smaller the value of  $\gamma$ , i. e. the greater  $l_\varphi$ , the greater is the average length of closed paths with a given area. For large area values  $S \gtrsim l^2$ , the area dependence of  $\bar{L}$  can be described by the power function  $S^\beta$  with  $\beta$  slightly depending on the value of  $\gamma$ . As  $\gamma$  changes from 0.1 to 0.01, the value of  $\beta$  varies from 0.55 to 0.62.

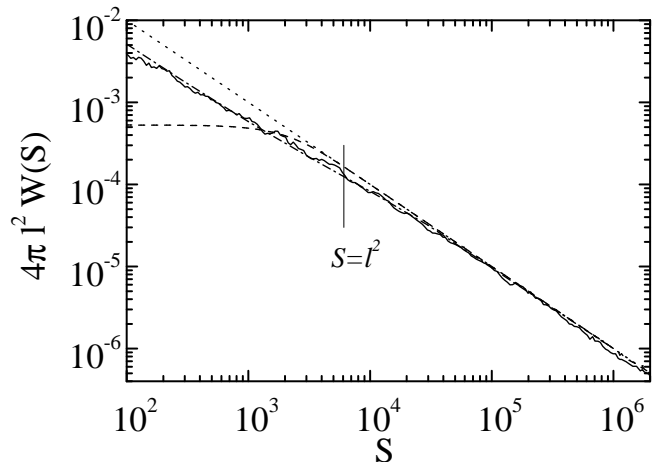


FIG. 3. Area distribution function of closed paths  $W(S)$ . The solid curve is the result of simulation; the dashed and dot-dashed curves are the diffusion and improved diffusion approximations, respectively; the dotted curve shows  $S^{-1}$  function.

Although the particle motion in our model 2D system is a special case of the random walker problem, which is studied well enough, to our knowledge there is no analytical solution of this problem in a wide range of path lengths and areas, involving non-diffusion motion. There is no theory which could describe analytically the statistics of closed paths with small number of collisions. Below we analyze the simulation results in the framework of diffusion theory.

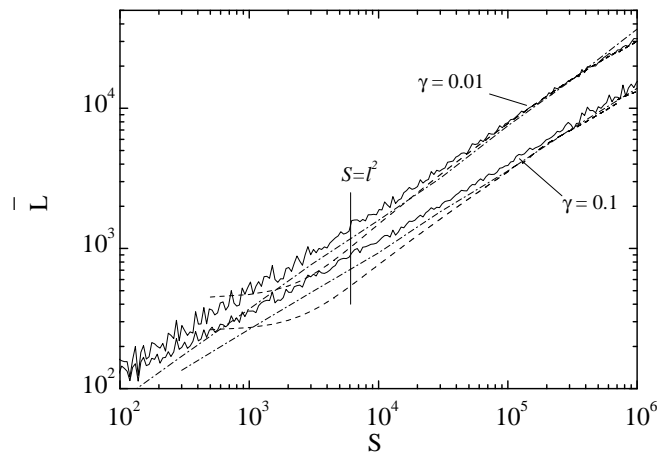


FIG. 4. The area dependence of  $\bar{L}$  for different  $\gamma$  values. Solid curves are the simulation results, dashed and dot-dashed curves are the results of calculation within the diffusion and improved diffusion approximations, respectively (see text).

## B. Comparison with diffusion theory

Let us now calculate within the diffusion approximation the quantities  $w(S, L)$ ,  $W(S)$ , and  $\bar{L}(S)$  introduced in Section II to describe statistical properties of a random

walk. A particle trajectory is regarded as being diffusive when its length is greater than the mean free path, associated with the transport scattering time. According to the diffusion theory the probability density of finding a particle in the vicinity of the point  $\mathbf{r}$  at the moment  $t$ ,  $P(\mathbf{r}, t)$ , does not depend on the initial and final velocity directions and obeys the usual diffusion equation

$$\frac{\partial P}{\partial t} - D\Delta P = \delta(t)\delta(\mathbf{r}), \quad (11)$$

where  $D$  is the diffusion coefficient. A solution of the diffusion equation can be written in the form of the Wiener path integral as (see, e.g. Ref. 2)

$$P(\mathbf{r}, t) = \int_{\mathbf{r}(0)=0}^{\mathbf{r}(t)=\mathbf{r}} \mathcal{D}\mathbf{r}(\tau) \exp\left(-\int_0^t d\tau \frac{\dot{\mathbf{r}}^2(\tau)}{4D}\right). \quad (12)$$

With help of this formalism we calculate the probability density  $\mathcal{P}$  for a diffusive walk with a constant velocity  $v_F$  and the length  $L = v_F t$  to enclose the algebraic area  $S$

$$\mathcal{P}(S, L) = \left\langle \delta\left(S - \frac{1}{2} \int_0^{t=L/v_F} d\tau r^2(\tau) \dot{\theta}(\tau)\right) \right\rangle_{P(0,t)}.$$

Here the symbol  $\langle \dots \rangle_{P(0,t)}$  stands for averaging with the Wiener measure (12) over all closed trajectories. The expression for  $\mathcal{P}(S, L)$  can be obtained by making use of relation between this quantity and density of states of a fictitious quantum particle with the mass  $m = \hbar(2D)^{-1}$  in a magnetic field:<sup>9</sup>

$$\mathcal{P}(S, L) = \frac{\pi}{2lL} \cosh^{-2}\left(\frac{\pi S}{lL}\right). \quad (13)$$

When obtaining Eq. (13) we have used the expression for the diffusion coefficient  $D = v_F^2 \tau / 2$ , and normalized  $\mathcal{P}(S, L)$  to unity:

$$\int_{-\infty}^{\infty} dS \mathcal{P}(S, L) = 1. \quad (14)$$

The function  $w(S, L)$ , which is connected with  $\mathcal{P}(S, L)$  through the diffusion density probability of return, by the following relationship

$$w(S, L) = \frac{1}{4\pi Dt} \mathcal{P}(S, L) = \frac{1}{2\pi lL} \mathcal{P}(S, L), \quad (15)$$

is shown in Fig. 5 for different  $L$  values. In the same figure the results of simulation are presented, too. As would be expected, the diffusion theory describes only the statistics of long trajectories (see corresponding curves labeled  $50l$  and  $500l$  in Fig. 5). For ballistic trajectories, there is no agreement between the simulation data and the above theory.

To calculate the function  $W(S)$ , which is given by the Eq. (7), we choose  $l$  as the lower cutoff in the integral, because the ballistic trajectories are not described within

the diffusion approximation. Using Eqs. (13) and (15) we immediately obtain

$$4\pi l^2 W(S) = \frac{1}{S} \tanh\left(\frac{\pi S}{l^2}\right). \quad (16)$$

In Fig. 3, the results of calculations of the function  $4\pi l^2 W(S)$  are presented by the dashed line. As is seen for large areas  $S > l^2$ , the simple diffusion theory describes the simulation results perfectly. For  $S < l^2$  the theory gives the values of  $W$  smaller than the simulation data.

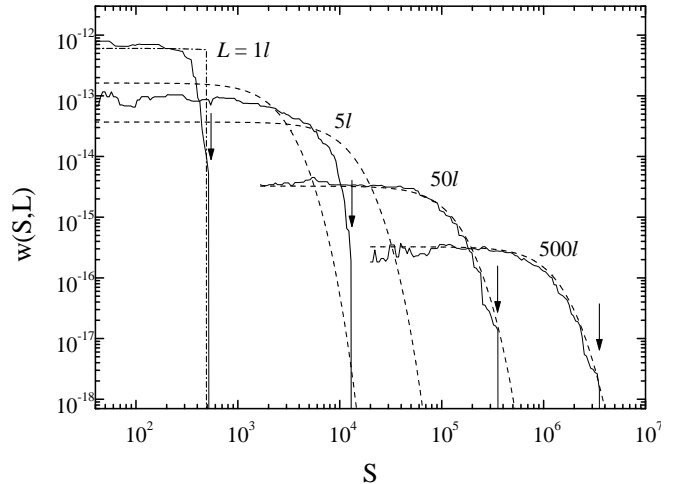


FIG. 5. The quantity  $w$  as a function of  $S$  for different  $L$  values. Solid lines represent the simulation data. Dashed and dot-dashed lines show the results of calculation using Eqs. (13) and (17), respectively. Arrows indicate the critical area value as it is obtained from the simulation procedure.

In the framework of the diffusion approximation we have calculated the area dependence of the average length of trajectories  $\bar{L}$ , introduced by Eq. (6). The results of numerical calculation are presented in Fig. 4 by the dashed curve. It is evident that the theoretical and simulation results are in good agreement only for  $S > 10l^2$ .

Let us suggest some improvement of the above theory, which could allow one to describe the statistic of ballistic trajectories as well. As is seen from Fig. 5, at some value of  $S = S_c$  (marked by arrows in Fig. 5) each curve obtained from the simulation procedure reveals a step-like behaviour: there are no paths with  $S > S_c$ . Such a behaviour of  $w(S, L)$  is quite clear. A closed path with the length  $L$  cannot enclose the area larger than the area of a circle with the radius  $L/(2\pi)$ . This fact, which has not been taken into account above, does not play an essential role within the diffusion regime, because the value of  $S_c$  is much greater than the area enclosed by almost all the trajectories. In the ballistic regime,  $S_c$  is found to be equal to the areas enclosed by the most probable trajectories (see Fig. 5, curves corresponding to  $L = 1l, 5l$ ). Not counting the existence of  $S_c$  in this case the function  $\mathcal{P}(S, L)$  (and  $w(S, L)$  too) is found to be underestimated

for  $S < S_c$  owing to the normalization of  $\mathcal{P}(S, L)$  according to Eq. (14). The artificial cutoff of the function  $\mathcal{P}(S, L)$  obtained in the framework of diffusion approximation (13) (i.e.  $\mathcal{P}(S, L) = 0$  for  $|S| > L^2/(4\pi)$ ) and following normalization (14) of this function gives

$$\mathcal{P}(S, L) = \frac{\pi}{2lL} \tanh^{-1} \left( \frac{L}{4l} \right) \times \cosh^{-2} \left( \frac{\pi S}{lL} \right) \Theta \left( \frac{L^2}{4\pi} - |S| \right) \quad (17)$$

where  $\Theta(x)$  is Heaviside step function. The use of this expression allows to describe  $w(S, L)$  behaviour for the ballistic trajectories much better than Eq. (13) (see the dash-dotted curve in Fig. 5). The results of numerical calculation of  $W(S)$  and  $\bar{L}(S)$  obtained in the framework of the improved theory are presented by the dash-dotted curves in Figs. 3 and 4, respectively. A good agreement with simulation results is evident for  $W(S)$  in the whole area range. However, such an approach is too rough to describe  $\bar{L}$ -vs- $S$  curves.

Thus, the theoretical analysis shows that the simulation procedure works correctly and allows to use it for analyzing, among other things, the interference quantum corrections to the conductivity.

## V. NEGATIVE MAGNETORESISTANCE

Before the discussion of negative magnetoresistance let us consider the results of calculation of  $\delta\sigma$  for  $b = 0$ . This will allow us to realize the restrictions of our model in view of the finite size of matrix used and limited number of collisions per one trajectory and to analyze for what  $\gamma$  range the simulation results can be applied to interpret experimental data for macroscopic samples (when the sample dimensions are much greater than the phase breaking length).

To calculate  $\delta\sigma$  we use Eq. (1) assuming that each closed path gives a contribution  $1/I_s$  (where  $I_s$  is a total number of paths) to the probability of return. Each contribution is weighted by the factor  $\exp(-l_i/l_\varphi)$  to take into account the interference distortion by inelastic processes. The final form of the expression for  $\delta\sigma$  in the case of  $b = 0$  looks as follows

$$\frac{\delta\sigma}{G_0} = -\frac{2\pi l}{I_s d} \sum_i \exp\left(-\frac{l_i}{l_\varphi}\right), \quad (18)$$

where summation runs over all closed trajectories. Figure 6 shows the results of our simulation of  $\delta\sigma$  as a function of  $\gamma = l/l_\varphi$  and, for comparison, the results of theoretical calculation obtained through the well known exact formula

$$\frac{\delta\sigma}{G_0} = \ln(1 + \gamma^{-1}). \quad (19)$$

As is seen for  $\gamma \gtrsim 10^{-2}$  the simulation and theoretical data are almost the same. A strong deviation is observed for  $\gamma < 10^{-3}$  where just the trajectories with lengths  $L \sim L_\varphi = \gamma^{-1} l > N_m l$  have to give an essential contribution to  $\delta\sigma$  value. These trajectories are not considered in our model. Thus, we believe that for  $\gamma = l/l_\varphi > 10^{-2}$  our model system is equivalent to an unbounded 2D system and the simulation gives correct results.

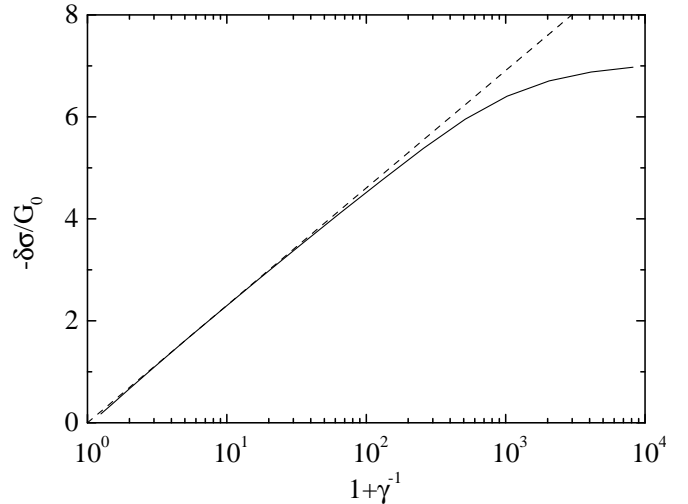


FIG. 6. The interference quantum correction to the conductivity in zero magnetic field as a function of  $\gamma$ . The solid curve shows the simulation results, the dashed line is the results of calculation according Eq. (19).

### A. Backscattering contribution

Now we are in position to discuss the magnetoconductance anomaly due to suppression of quantum interference corrections by a magnetic field. To calculate a magnetic field dependence of  $\delta\sigma$  for our model system we follow the ordinary way: the contribution of each closed trajectory to  $\delta\sigma$  is multiplied by the factor, which allows for the interference distortion by the magnetic field. The final expression for  $\delta\sigma(b)$  takes the form:

$$\frac{\delta\sigma(b)}{G_0} = -\frac{2\pi l}{I_s d} \sum_i \cos\left(\frac{(1 + \gamma)^2 b S_i}{l^2}\right) \exp\left(-\frac{l_i}{l_\varphi}\right). \quad (20)$$

This formula is not meaningful from the experimental point of view, because the absolute value of quantum correction is not a measurable quantity. The magnetoconductance  $\Delta\sigma(b) = \sigma(b) - \sigma(0) = \delta\sigma(b) - \delta\sigma(0)$  is usually experimentally available.

The results of calculation of  $\Delta\sigma(b)$  for the model system are presented in Fig. 7 for several  $\gamma$  values. They are in excellent agreement with the results of numerical calculations carried out beyond the diffusion approximation in Ref. 5. This lends support to the correctness of parameters chosen for our model system: the set of parameters used turns out to be suitable to simulate adequately  $\Delta\sigma(b)$  in the ranges of  $b$  and  $\gamma$  under consideration.

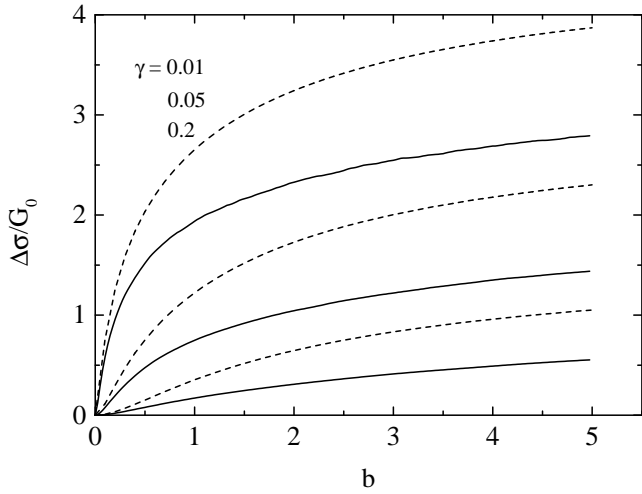


FIG. 7. The magnetic field dependence of  $\Delta\sigma$  for different  $\gamma$  values. Solid curves are the results of simulation, dashed curves are the diffusion limit (3). Only backscattering contribution is taken into account.

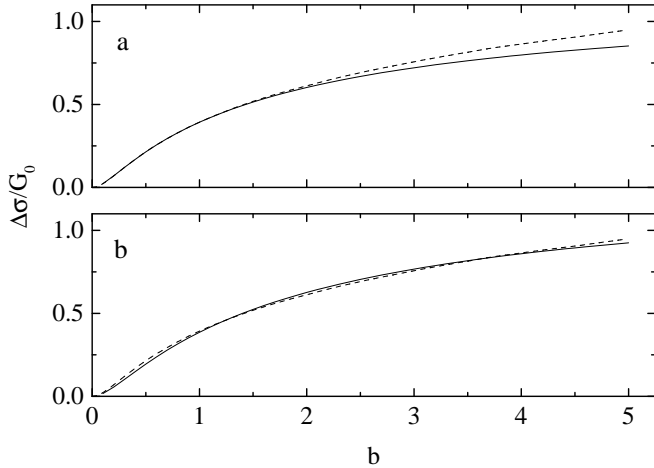


FIG. 8. The magnetic field dependence of  $\Delta\sigma$  for  $\gamma = 0.1$ . Solid curves are the results of simulation. Dashed curves are the results of fitting procedure with the use of Eq. (3) made within two different ranges of magnetic field:  $b \leq 1$  (a) and  $b \leq 5$  (b). The fitting parameters are the following:  $a = 0.49$ ,  $\gamma_f = 0.087$  (a) and  $a = 0.65$ ,  $\gamma_f = 0.12$  (b).

In the same figure the results of calculation of  $\Delta\sigma(b)$  in the framework of diffusion approximation with the expression (3) are presented too. It is seen that this formula does not describe the simulated  $\Delta\sigma(b)$  curves. Even in the case of  $\gamma = 0.01$ , when the condition  $\gamma \ll 1$  is seemingly fulfilled and the diffusion theory should work well, the formula (3) gives the value of  $\Delta\sigma$  substantially larger than the simulation data: for  $b = 0.1$  the difference is about 25%.

As discussed above (see Section I) Eq. (3) is widely used by experimenters to extract the values of  $\gamma$  from experimental data. Two fitting parameters are available in such a data processing: just as the value of  $\gamma$  so the

prefactor  $a$ . To check the validity of this method in the case when the diffusion approximation does not work, we have performed the fitting procedure for  $\Delta\sigma(b)$  curves simulated. In Fig. 8 the results of fitting procedure of  $\Delta\sigma(b)$  made for  $\gamma = 0.1$  within two different ranges of magnetic field  $b \leq 1$ , and  $b \leq 5$  are presented by dotted and dashed curves, respectively. As is seen the simulated curve is best described by Eq. (3) in low magnetic field range. However in both cases the ratio  $\tau/\tau_\varphi$  found from the fitting procedure and designated as  $\gamma_f$  slightly differs from the value of  $\gamma$  used in the simulation. The difference is about 10% for  $b \leq 1$  fitting range and 20% for  $b \leq 5$ . The value of prefactor is found to be significantly less than unity.

The results of such a data treatment for several  $\gamma$  values are presented in Fig. 9. It is clearly seen that the difference 10..30% between  $\gamma_f$  and  $\gamma$  takes place for all  $\gamma$  values. The value of prefactor  $a$  is always less than unity, and increases with decreasing  $\gamma$ .

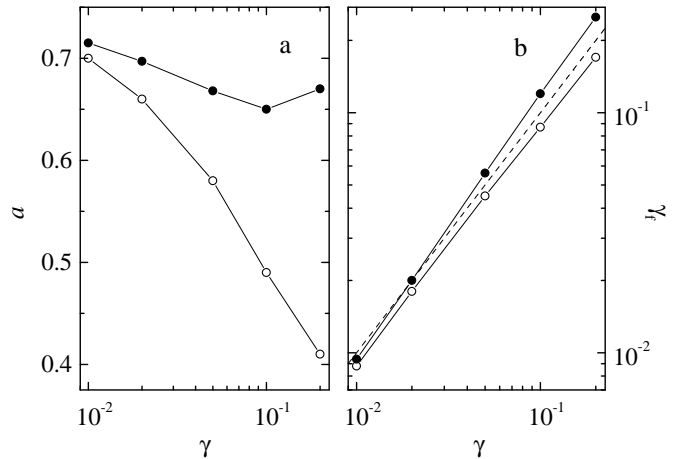


FIG. 9. The parameters  $a$  (a) and  $\gamma_f$  (b) as a function of  $\gamma$  value fed into the simulation. Open and solid circles are the results of fitting of  $\Delta\sigma(b)$ , obtained without non-backscattering contribution, to Eq. (3) in the ranges  $b \leq 1$  and  $b \leq 5$ , respectively. Solid lines are the guide for an eye, the dashed line shows  $\gamma = \gamma_f$  function.

## B. Nonbackscattering contribution

Up to this point we considered the coherent backscattering correction to conductivity. The coherent paths for backscattering contribution are schematically depicted in Fig. 10a. In this case the interference takes place when the points  $A$ ,  $1$ ,  $N$  and  $B$  are close to one line. However as it is shown in Ref. 4 there is one more variant of coherent paths for the same configuration of scatterers, when the finish point  $B$  lies close to the line passing through the points  $1$  and  $2$  (see Fig. 10b). In the latter case the one of the two interfering waves is scattered twice by the scatterer  $1$  (which is regarded in this paper as a starting point), while the other one passes the point  $1$  without scattering. This provides so called nonbackscattering

contribution to conductivity. It was shown in<sup>4</sup> that both contributions are related to the probability of return to the starting point for a given trajectory, the conductivity correction due to nonbackscattering processes is positive. In our case such processes can be easily taken into account by multiplying each term in Eq. (20) by the factor  $(1 - \cos(\theta_i))$ , where  $\theta_i$  is the angle between the first and last segments of the  $i$ -th closed path:

$$\frac{\Delta\sigma(b)}{G_0} = -\frac{2\pi l}{I_s d} \sum_i [\dots] (1 - \cos(\theta_i)). \quad (21)$$

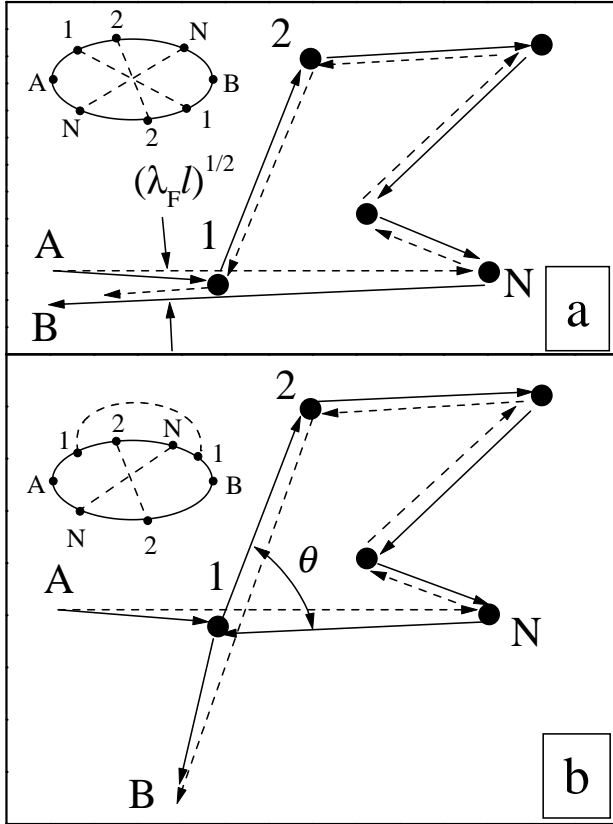


FIG. 10. Two types of coherent paths and corresponding diagrams relevant in the first order in  $(k_F l)^{-1}$ , which are responsible for backscattering (a) and nonbackscattering (b) contributions to weak localization, for given configuration of scatterers.

Shown in Fig. 11 are the magnetic field dependencies of  $\Delta\sigma$ , calculated for different  $\gamma$  values with the help of Eq. (21). For comparison, the results computed with the formula (20) are presented too. It is clearly seen that both types of calculations give close results in the low magnetic field range  $b \lesssim 0.5$ . For higher magnetic fields the inclusion of nonbackscattering contribution leads to a decrease in magnetoconductance. Such a behaviour of the magnetoconductance is in a good agreement with the results of numerical calculations presented in Ref. 4.

As in the previous subsection we have attacked the

simulated data as experimental ones, i.e.  $\Delta\sigma(b)$  curves have been fitted to the calculated with Eq. (3) values. The fitting results are presented in Fig. 12. As one would expect, the values of  $a$  and  $\gamma_f$  obtained from the low magnetic field fitting ( $b \leq 1$ ) are very close to corresponding values in Fig. 9. This obviously results from the fact that the solid and dashed curves in Fig. 11 are close together for these  $b$  values. As for the parameters obtained from the whole magnetic field range fitting, taking into account of the nonbackscattering contribution results in decreasing both  $a$  and  $\gamma_f$  values.

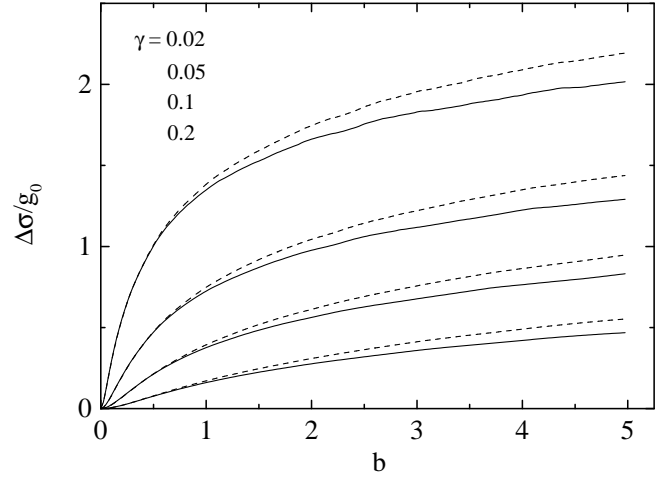


FIG. 11. The magnetic field dependence of  $\Delta\sigma$  for different  $\gamma$  values. Dashed and solid curves are the results of calculation without and with non-backscattering contribution, respectively.

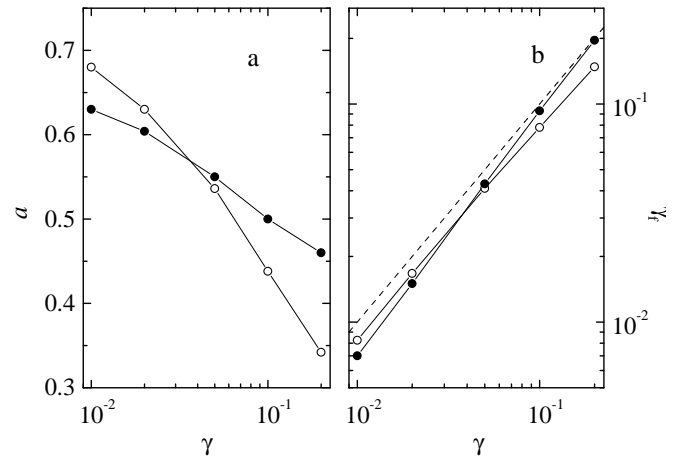


FIG. 12. The parameters  $a$  (a) and  $\gamma_f$  (b) as a function of  $\gamma$  value fed into the simulation. Non-backscattering contribution is taken into account. All designations are the same as in Fig. 9.

Thus, the standard method of experimental data processing with the use of Eq. (3) allows to extract the phase breaking time (or length) with the accuracy (10 – 30) %



in wide ranges of  $\gamma$  and  $b$ . The prefactor  $a$  obtained this way is found to take the values from 0.3 to 0.7, i.e. substantially less than unity. This reveals a possible reason of small value of prefactor obtained from different experimental data treatment. This need not be a consequence of an electron-electron interaction as discussed in some papers, but can result from the fact that in real 2D systems the rigorous conditions of diffusion approximation are not fulfilled even in the case of rather small  $\gamma$  and  $b$ .

## VI. CONCLUSION

This paper is intended to demonstrate the possibility of obtaining the information about the statistics of closed paths from the analysis of anomalous magnetoconductance in 2D systems. In particular we have shown explicitly that the statistic characteristics such as the area distribution function of closed paths and area dependence of their average lengths determine the magnetic field dependence of magnetoconductance. These functions have been studied by using the computer simulation method. It has been shown that in the ballistic regime the area distribution function of closed paths deviates from  $S^{-1}$  power law, which holds in the diffusion regime. The theoretical analysis of simulation results has shown that such a behaviour of  $W(S)l$  is mainly connected with the existence of critical area value, which corresponds to the maximal area enclosed by a path with a fixed length. It has been shown that the area dependence of the average length of closed paths, introduced through Eq. (6), can be well described by the power function,  $\bar{L} \propto S^\beta$ , with  $\beta$  varying in the range 0.55 – 0.62, when  $\gamma = \tau/\tau_\varphi$  changes from 0.1 to 0.01.

The results of simulation have been used to calculate the magnetoresistance of the model 2D system. Both backscattering and nonbackscattering processes have been taken into account. The calculated magnetic field dependencies of  $\Delta\sigma$  have been processed as experimental ones by a standard manner with the help of Eq. (3). It has been shown that the fitting procedure gives  $\tau/\tau_\varphi$  ratio, which differs from that used in the simulation by the factor 0.8 – 1.3. The value of prefactor obtained this way is always less than unity.

## Acknowledgments

We thank A.P. Dmitriev, V.Yu. Kachorovskii, and A.G.Yashenkin for useful discussions. This work was supported in part by the RFBR through Grants 97-02-16168, 98-02-17286, and 99-02-17110, the Russian Program *Physics of Solid State Nanostructures* through Grant 97-1091, INTAS through Grant 97-1342 and the Program *University of Russia* through Grant 420.

## APPENDIX

For the sake of simplicity we suppose here that the start point coincides with the origin. For the value of probability  $\mathcal{T}$  that a trajectory passes near the origin at the distance less than some prescribed value  $d/2$  we can write

$$\mathcal{T} = \sum_{N=3}^{N_m} \mathcal{T}_N, \quad (22)$$

where  $\mathcal{T}_N$  is the probability of return after  $N$  collisions. The value of  $\mathcal{T}_N$  can be expressed through the probability density to experience the  $(N-1)$ -th collision in the point  $\mathbf{r}$ ,  $W_{N-1}(\mathbf{r})$ :

$$\mathcal{T}_N = \int d\mathbf{r} \mathcal{P}(r) W_{N-1}(\mathbf{r}), \quad (23)$$

where  $\mathcal{P}(r)$  is the probability that the particle moves without collisions from the point  $\mathbf{r}$  to the circle of the radius  $d/2$  around the origin. It is easy to show that

$$\mathcal{P}(r) = \frac{1}{\pi} \arctan\left(\frac{d}{2r}\right) \exp\left(-\frac{r}{l}\right). \quad (24)$$

Then, for  $\mathcal{T}_N$  we have

$$\mathcal{T}_N = \frac{1}{\pi} \int d\mathbf{r} \arctan\left(\frac{d}{2r}\right) \exp\left(-\frac{r}{l}\right) W_{N-1}(\mathbf{r}). \quad (25)$$

For  $d \ll l$ , the inverse tangent in Eq. (25) can be replaced by its argument. Analysis shows that for  $d/l = 10^{-2}$  (it is true for our case) this gives an error in calculation of  $\mathcal{T}_N$  less than 0.1 % for  $N \geq 3$ . Thus the expression for the probability  $\mathcal{T}$  becomes

$$\mathcal{T} \simeq \frac{d}{2\pi} \sum_{N=3}^{N_m} \int \frac{d\mathbf{r}}{r} \exp\left(-\frac{r}{l}\right) W_{N-1}(\mathbf{r}). \quad (26)$$

Comparing Eq. (26) with the expression for the probability density  $W^{3,5}$

$$W = \frac{1}{2\pi l} \sum_{N=3}^{N_m} \int \frac{d\mathbf{r}}{r} \exp\left(-\frac{r}{l}\right) W_{N-1}(\mathbf{r}), \quad (27)$$

we can conclude that

$$W \simeq (ld)^{-1} \mathcal{T}. \quad (28)$$

---

\* Email: Alexander.Germanenko@usu.ru, ICQ: 46042648

<sup>1</sup> L. P. Gorkov, A. I. Larkin, D. E. Khmel'nitskii, JETP Lett. **30**, 248 (1979).

- <sup>2</sup> S. Chakravarty and A. Schmid, Phys. Reports **140**, 193 (1986).
- <sup>3</sup> M. I. Dyakonov, Solid St. Comm. **92**, 711 (1994).
- <sup>4</sup> I. V. Gornyi, A. P. Dmitriev, and V. Yu. Kachorovskii, Phys. Rev. B **56**, 9910 (1997).
- <sup>5</sup> H.-P. Wittman and A. Schmid, J. Low. Temp. Phys. **69**, 131 (1987).
- <sup>6</sup> S. Hikami, A. Larkin and Y. Nagaoka, Prog. Theor. Phys. **63**, 707 (1980).
- <sup>7</sup> D. Rainer and G. Bergmann, Phys. Rev. B **32**, 3522 (1985).
- <sup>8</sup> The bending of the trajectory in a magnetic field due to Lorentz force is neglected provided that the cyclotron radius is much greater than the mean free path. This condition corresponds to the requirement  $k_F l / b \gg 1$ . Since all the theory of weak localization is true when  $k_F l \gg 1$  the above condition is well justified in the whole range of magnetic fields under study throughout this paper ( $b < 5$ ).
- <sup>9</sup> K. V. Samokhin, Phys. Rev. E **59**, 2501R (1999).